A STRUCTURED APPROACH TO AUTOMATED CRATER DETECTION. J. Saraiva, L. P. C. Bandeira and P. Pina, CVRM/Centro de Geo-Sistemas, Instituto Superior Técnico, Av. Rovisco Pais, 1049 – 001 Lisboa, Portugal. E-mail: jsaraiva@alfa.ist.utl.pt, lpcbandeira@ist.utl.pt, ppina@alfa.ist.utl.pt.

Introduction: A structured methodology aimed at the automated recognition of impact craters on planetary surfaces is presented. The initial phase focus on edge detection; this is followed by a crucial step, in which a template matching procedure is employed to create a probability volume from which the best candidates are selected and undergo a third phase, designed to detect the centers and estimate the dimensions (radius) of craters which are then plotted on the images.

Methodology: The approach we present proceeds according to a similar scheme, used by other workers in this field [1-5]. It comprises three main phases, which are shortly described below (for a fuller description, see [6, 7]), and illustrated in figure 1 through their sequential application to a MOC/MGS wide angle image (figure 1 (a)).

Edge detection. In this phase the objective is to identify, in the scene image, regions that correspond to crater rims. To achieve this goal we use an edge detection operator which incorporates local information and thus constitutes an improvement relative to classic edge detectors. The result is a binary image that will serve as input for the next phase of the method (figure 1 (b)).

Template matching. This process involves cross-correlating a template with the scene image and computing a measure of similarity between them. The template employed in this work is a simple black and white circular crater model (see figure 1), suited to the binary image that resulted from the edge detection. The Fast Fourier Transform, a proven method applied in the frequency domain, was used for the actual computation of the correlation between the scene image and the series of templates with different sizes. The values (one per pixel and per template dimension) are normalized and collected into a probability volume (figure 1 (c)), a stack of r planes (r being the range of values used for template radius) each containing u x v pixels (the size of the image).

Crater recognition. Assuming that a crater produces an identifiable signature on the probability volume, we look for all the local probability maxima and sort them out in a number of steps involving the analysis of their neighborhoods according to morphological features (dimension and roundness are considered). The end result of this cyclic process (which runs as many times as there are planes in the probability volume) is the elimination of weaker candidates and the identification of the probable centers of craters, along with the corresponding radius (figure 1 (d)).

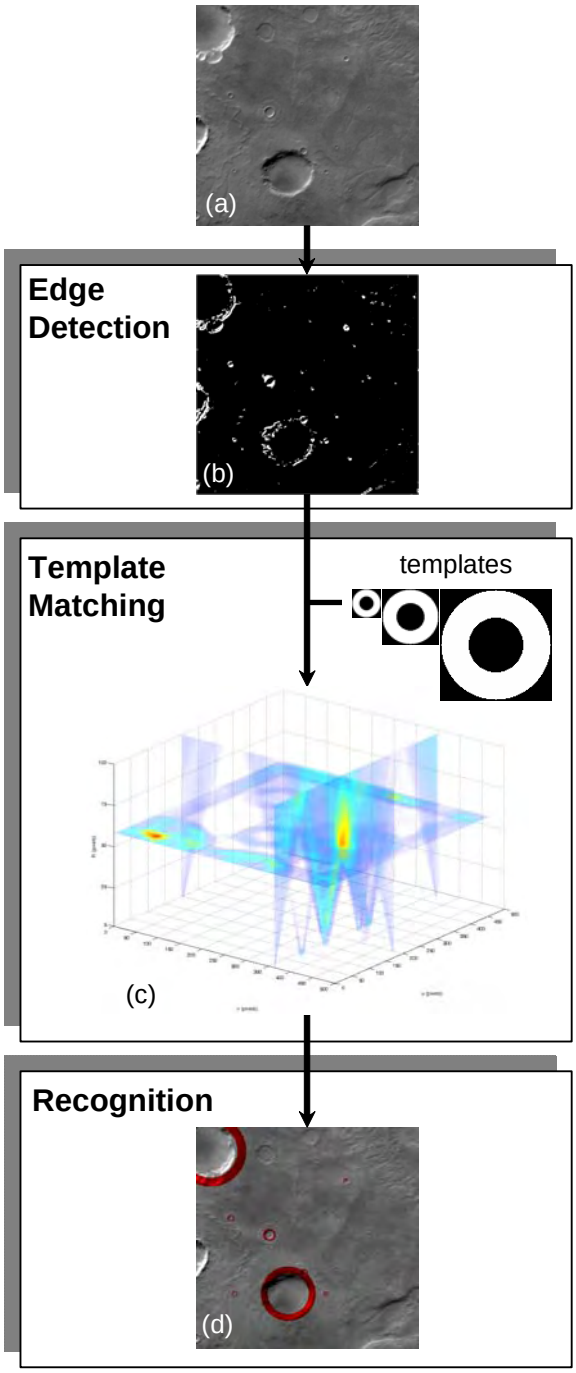

Figure 1. Proposed three-phased sequence to recognize impact craters. The original image is E1900566 (NASA/JPL/MSSS), with a spatial resolution of 245 m/pixel.

Results: The methodology was applied to a set of 26 images obtained by MOC/MGS. These wide angle images with a spatial resolution of about 245 m/pixel cover approximately 350000 km^2 and were selected from different regions of the planet in order to sample different geomorphological settings. The global results can be seen in Table 1.

Table 1. Recognition rates obtained

Craters	Detection	
	Visual	Automatic
Recognised (#)	252	158
False (#)	-	32

On average, 63% of the 252 craters with radius between 1.2 km (5 pixels) and 24.5 km (100 pixels) that we identified on all images were correctly detected, a result that can be regarded as very satisfactory, considering the differing characteristics of the areas imaged and the use of the same set of parameters for all images. Moreover, more than 50% of the images showed a recognition rate higher than 67%. Our approach also shows a very low number of false positives; on 11 of the 26 images there were no false detections. Since this is a problem that plagues all the approaches to the issue under consideration, we believe that these results can be considered as major improvements.

On figure 2 we can see five examples of crater detection on MOC images. Figure 2 (a) shows an uncluttered scene where 7 of the 9 visually identified craters were automatically recognized (78%). Note that the large scale structure on the bottom centre of the image does not induce the creation of false positives. The scene captured on figure 2 (b) is dominated by the presence of channels and the contrasting surface tone; again, no false positives occur, and 9 out of 13 craters were correctly detected (69%). The somewhat poor contrast evident in the image on figure 2 (c) did not prevent our methodology from obtaining excellent results, with 7 out of 8 craters detected (88%) and no false positives, despite the presence of a rounded feature on the bottom right that could be easily mistaken for a crater. On figure 2 (d), it must be noted that the rim of the largest crater, being a highly cluttered area, produced a false positive (in green). Notwithstanding, the rate of detection was 89% (16 in 18 craters). Finally, figure 2 (e) shows a scene with large scale arcuate structures, similar to the one present on figure 2 (a), and the results are comparable, 8 out of 11 craters detected (73%) and no false positives.

To conclude, the methodology presented was applied to several regions of the surface of Mars and proved itself to be a robust approach, both in what concerns recognition rates and low production of false positive craters.

Future Work: We intend to continue with the development of this approach, using more complex templates that better reflect the true appearance of impact craters on the scene image. We expect that this will lead to even better recognition rates.

References: [1] Leroy B. (2001), *Image & Vis. Comp. (19)*, 787-792. [2] Vinogradova T. (2002) *IEEE Aerospace Conf. (7)*, 3201-3211. [3] Magee M. (2003) *LPS XXXIV*, abs #1756. [4] Plesko C. et al. (2004) *LPS XXXV*, abs #1935. [5] Kim J. R. et al. (2005) *PE&RS, 71*, 1205-1217. [6] Bandeira L. et al. (2006) *VISAPP 06 (accepted).* [7] Bandeira L. et al. (2006) *ICPR 06 (submitted).*

Acknowledgements: This work was developed in the frame of the project PDCTE/CTA/49724/03.

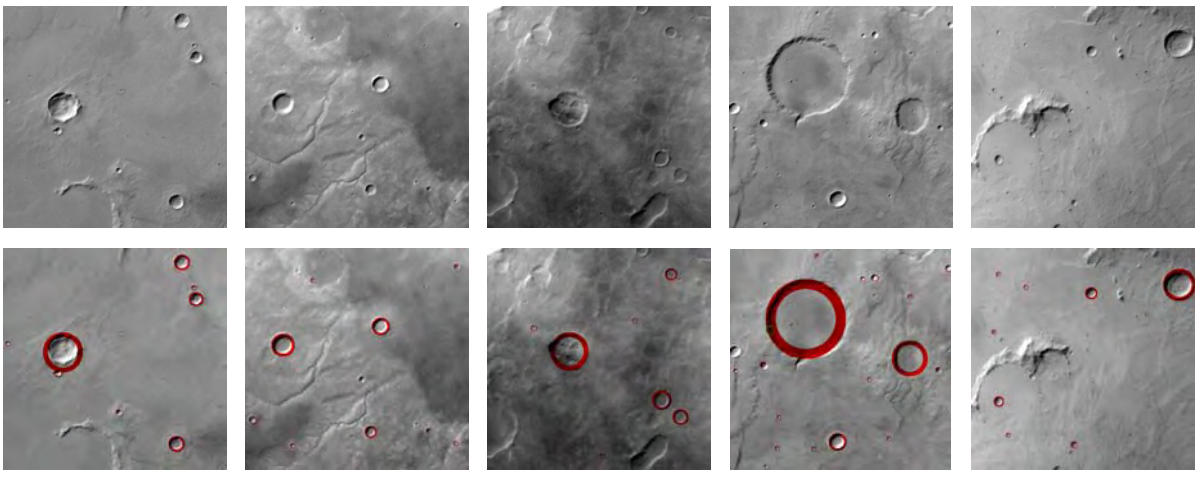

Figure 2.

(a) R0101374 (b) R0200575 (c) R0200830 (d) R0200837 (e) R0200872

(NASA/JPL/MSSS)